

From zero resistance states to absolute negative conductivity in microwave irradiated 2D electron systems

J. Iñarrea^{1,2} and G. Platero¹

¹*Instituto de Ciencia de Materiales, CSIC, Cantoblanco, Madrid, 28049, Spain*

²*Escuela Politécnica Superior, Universidad Carlos III, Leganes, Madrid, 28911, Spain*

(Dated: June 24, 2018)

Recent experimental results regarding a 2D electron gas subjected to microwave radiation reveal that magnetoresistivity, apart from presenting oscillations and zero resistance states, can evolve to negative values at minima. In other words, the current can evolve from flowing with no dissipation, to flow in the opposite direction of the dc bias applied. Here we present a theoretical model in which the existence of radiation-induced absolute negative conductivity is analyzed. Our model explains the transition from zero resistance states to absolute negative conductivity in terms of multiphoton assisted electron scattering due to charged impurities and shows how this transition can be driven by tuning microwave frequency and intensity. This opens the possibility of controlling the magnetoconductivity in microwave driven nanodevices and understanding the novel optical and transport properties of such devices.

PACS numbers:

The effect of an AC field on the electronic transport properties of nanostructures has been an active research topic in the last years. One reason for this is that the AC field can profoundly modify the electronic structure and the dynamical properties of electrons in the nanostructure. The application of an external AC potential also allows the electronic properties to be tuned in a controllable way^{1,2}. Ten years ago, transport experiments on AC-driven weakly coupled semiconductors superlattices revealed a fascinating, non-intuitive, behavior: for certain parameters of the AC potential and stationary electric field, the electronic current flowed *uphill* presenting absolute negative conductivity (ANC)³. In the rapid developing field of nanoelectronics, it can be expected that nanodevices, will soon routinely incorporate two-dimensional electron systems. A deep knowledge of how this structures respond to external electromagnetic fields is thus of high importance.

Recently two experimental groups^{4,5} have announced the existence of oscillations and zero resistance states (ZRS) in the longitudinal magnetoresistivity (ρ_{xx}) of two dimensional electron systems (2DES) subjected to microwave (MW) radiation and a perpendicular magnetic field (B). One of the most controversial topics in this field, has been the existence of ANC and even the very presence of ZRS has been also questioned. Most experimental works^{4,5,6,7,8,9,10,11}, report clearly such vanishing dissipation states but not ANC. Only Willett et al¹², and very recently Zudov et al¹³, have reported minima in which ρ_{xx} is distinctly negative. On the other hand many theoretical contributions have been presented to explain ρ_{xx} oscillations with B and the possibility of ZRS and ANC^{14,15,16,17,18,19,20,21,22,23,24,25}.

Here we present a microscopical model which explains how the system evolves from ZRS to ANC. The proposed theory is based on how the Larmor orbits dynamics are driven by the MW field and the external DC bias (E_{DC}) in the transport direction (x -direction). It shows how

this transition can be driven by tuning the MW parameters. We start from an exact expression for the electronic wave function dressed by photons. This many body wave function is expressed in terms of photosatellites and energy sidebands^{26,27}. At high MW-power and low frequency, multi-photon processes become relevant in assisting electron-charged impurity scattering, responsible for ρ_{xx} . This exact solution for the electronic wave function of a 2DES in a perpendicular B -field, a DC electric field and MW radiation, is given by^{23,28,29}:

$$\Psi(x, t) \propto \phi_n(x - X - x_{cl}(t), t) \sum_{p=-\infty}^{\infty} J_p \left[\alpha \frac{eE_0 X}{\hbar w} \right] e^{ipwt} \quad (1)$$

where e is the electron charge, ϕ_n is the solution for the Schrödinger equation of the unforced quantum harmonic oscillator, w the MW frequency, E_0 the intensity for the MW field, X is the center of the orbit for the electron motion, $x_{cl} = A \cos wt$ where $A \propto \frac{eE_0}{m^* w^2}$ and J_p are Bessel functions. The wave function includes the energy sidebands $\epsilon_n, \epsilon_n \pm \hbar w, \epsilon_n \pm 2\hbar w, \dots, \epsilon_n \pm p\hbar w$ and shows that, due to the MW radiation, the centers of electronic orbits are not fixed, but instead oscillate back and forth harmonically with w and amplitude A . Electrons suffer scattering due to charged impurities that are randomly distributed in the sample. To proceed we calculate the electron-charged impurity multi-photon assisted transition rate $W_{n,m}$, from an initial state $\Psi_n(x, t)$, to a final state $\Psi_m(x, t)$ ³⁰: $W_{n,m} = W_{n,m}(0)[B_0 + B_1 + B_2]$ where,

$W_{n,m}(0)$ is the transition rate when $J_0 \simeq 1$, and

$$B_0 = [J_0^2(A_m)J_0^2(A_n) + \sum_1^s 2J_s^2(A_m)J_s^2(A_n)] \times \left[\frac{\Gamma}{[\hbar\omega_c(n-m)]^2 + \Gamma^2} \right] \quad (2)$$

$$B_1 = \left[\sum_0^s J_s^2(A_m)J_{s+1}^2(A_n) + J_{s+1}^2(A_m)J_s^2(A_n) \right] \times \left[\frac{\Gamma}{[\hbar\omega_c(n-m) + \hbar\omega]^2 + \Gamma^2} \right] \quad (3)$$

$$B_2 = [J_1^2(A_m)J_1^2(A_n) + \sum_0^s J_s^2(A_m)J_{s+2}^2(A_n) + J_{s+2}^2(A_m)J_s^2(A_n)] \times \left[\frac{\Gamma}{[\hbar\omega_c(n-m) + 2\hbar\omega]^2 + \Gamma^2} \right] \quad (4)$$

Here $A_i \propto \frac{E_0}{w} 2^3$ and Γ is the state (Landau level) broadening due to different scattering mechanisms. Multiphoton processes have been considered up to 2 photons.

The average effective distance advanced by the electron in every scattering jump is given by: $\Delta X^{MW} = \Delta X^0 + A \cos w\tau$, where ΔX^0 is the effective distance advanced when there is no MW field present and $1/\tau = W_{n,m}$ (τ being the impurity scattering time). From here, the longitudinal conductivity σ_{xx} can be calculated through $\sigma_{xx} \propto \int \rho(E_n) \frac{\Delta X^{MW}}{\tau} (f_i - f_f) dE_n$, where f_i and f_f are the distribution functions for the initial and final Landau states respectively:

$$\sigma_{xx} = \sigma_{xx}(0)[B_0[f(E_n) - f(E_m)] + B_1[f(E_n) - f(E_m + \hbar\omega)] + B_2[f(E_n) - f(E_m + 2\hbar\omega)]] \quad (5)$$

and $\sigma_{xx}(0)$ is the conductivity when $J_0 \simeq 1$. To obtain ρ_{xx} we use the relation $\rho_{xx} = \frac{\sigma_{xx}}{\sigma_{xx}^2 + \sigma_{xy}^2} \simeq \frac{\sigma_{xx}}{\sigma_{xy}^2}$, where $\sigma_{xy} \simeq \frac{n_i e}{B}$ and $\sigma_{xx} \ll \sigma_{xy}$.

In Fig. 1 the calculated ρ_{xx} as a function of B for different MW power at fixed frequency $\nu = w/2\pi = 70GHz$ is shown. Our results follow the qualitative experimental behavior¹², and show that ANC occurs at the principal minimum, as the incident radiation power is increased. The inset shows the evolution from ZRS to negative conductivity. The physical explanation is as follows. In Fig. 2 we represent schematic diagrams to describe ρ_{xx} evolution at minima. In Fig. 2a orbits are moving forwards and on average the electron advances a shorter distance than in the no MW case, $\Delta X^{MW} < \Delta X^0$. This corresponds to a decrease in the conductivity but $\rho_{xx} > 0$ still. If we raise the MW power we will eventually reach the situation depicted in Fig. 2b, where orbits are moving forwards but their amplitude A is larger than the electronic jump. In this case the jump is blocked by the Pauli exclusion principle because the final state is occupied. *This is the physical origin of the ZRS*. At fixed pho-

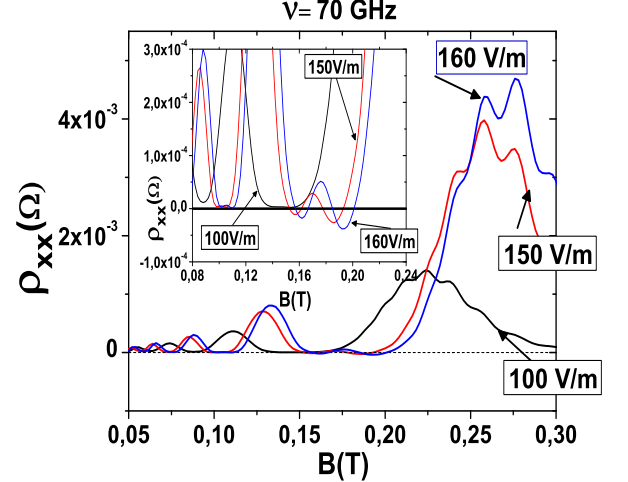


FIG. 1: Calculated magnetoresistivity ρ_{xx} as a function of B , for different MW-intensities at $\nu = 70GHz$. In the inset we show amplifications of principal minima. Zero resistance states, absolute negative conductivity and the corresponding evolution for increasing MW-power can be observed Temperature: 500 mK.

ton frequency, small values for MW-power correspond to transitions where no photon absorption or emission are involved, i.e., the arguments of Bessel functions are so small that only J_0 terms need to be taken into account. This implies that only direct, $J_0 \rightarrow J_0$, transitions are relevant. This corresponds to Fig. 2a and 2b. If we further increase the MW-power, while keeping the frequency constant, the argument of the Bessel functions will become larger, and higher order sidebands must be considered: multi-photon transitions become relevant. Transitions such $J_1 \rightarrow J_0$ and $J_2 \rightarrow J_0$, which correspond to one photon and two photons processes respectively, can then play an effective role in the current. At minima and for A larger than the electron scattering jump (large MW-power), we find a situation where $\Delta X^{MW} < 0$. However for multi-photon transitions $J_1 \rightarrow J_0$ or $J_2 \rightarrow J_0$ etc, the difference of distribution functions $(f_i - f_f) > 0$. These processes ($\Delta X^{MW} < 0$ and $(f_i - f_f) > 0 \Rightarrow \rho_{xx} < 0$) produce negative contributions to the current and *are the physical origin of ANC*.

One surprising effect in the experimental results is the positive peak in the middle of ρ_{xx} negative minimum. This is also observed in calculated results. (see inset of Fig. 1). The explanation for this can be readily obtained. In a regime with $\Delta X^{MW} < 0$ and finite temperature, direct ($J_0 \rightarrow J_0$) transitions, can correspond to negative values for the difference of electronic distribution functions, $(f_i - f_f)$. This is due to the fact that in such a regime, the final state is always deeper in energy than the initial state, with respect to the Fermi energy. Considering the smearing of the distribution

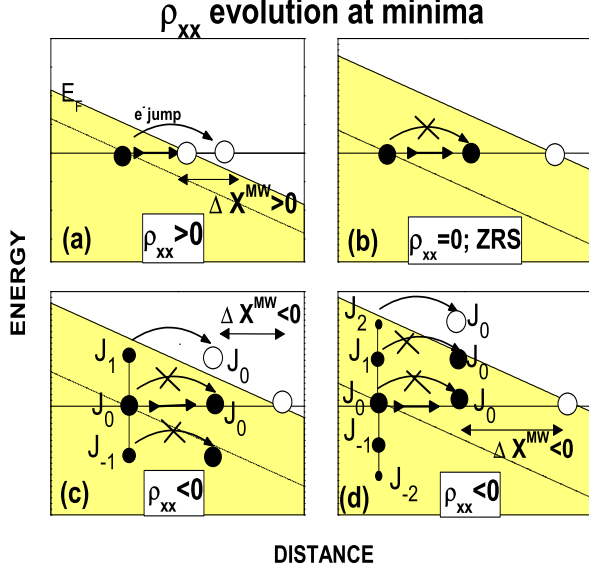


FIG. 2: Schematic diagrams of electronic transport describing ρ_{xx} evolution at minima, for fixed MW frequency and different MW intensities. When the MW-field is on, electronic orbits oscillate with w and at minima, displacement is forwards. In (a) the average distance advanced by the electron ΔX^{MW} is shorter than the no MW case ΔX^0 ($\Delta X^{MW} < \Delta X^0$). This corresponds to a reduction in the conductivity but still $\rho_{xx} > 0$. In (b), at higher intensity we can reach a situation where the amplitude A , of the electronic orbit oscillations, is larger than electronic jump, and the electronic movement between orbits cannot take place because the final state is occupied. This situation corresponds to ZRS and $\rho_{xx} \sim 0$. In (c) and (d) due to further increases in MW-power the wave function sidebands play and important role. In (c) one photon, $J_1 \rightarrow J_0$, transitions can take place giving rise to negative conductivity ($\Delta X^{MW} < 0$ and $(f_i - f_f) > 0 \Rightarrow \rho_{xx} < 0$). In (d) the negative contribution transition corresponds to two photons, $J_2 \rightarrow J_0$, transitions also giving $\rho_{xx} < 0$.

function at finite temperature, the final result is that $f_i < f_f \Rightarrow (f_i - f_f) < 0$.

When $\Delta X^{MW} < 0$ and $(f_i - f_f) < 0$, an effective positive net current will be produced giving rise to a positive ρ_{xx} . In the inset of Fig. 1 it can also be observed that an increase in MW-power produces an increase in the positive and negative part of the minimum in a similar way. The explanation has to do with the corresponding increase in the amplitude A and, as a consequence, in ΔX^{MW} . This has a similar impact on both the one-photon, $J_1 \rightarrow J_0$, transitions (negative contributions) and on the direct $J_0 \rightarrow J_0$ ones, (positive contributions). Positive net values for ρ_{xx} in the middle of the main minima, have been experimentally obtained by other groups^{7,12}, notably in ref [7], where this effect was termed "breakdown of ZRS".

Fig. 3 shows ρ_{xx} versus B for different MW-frequencies

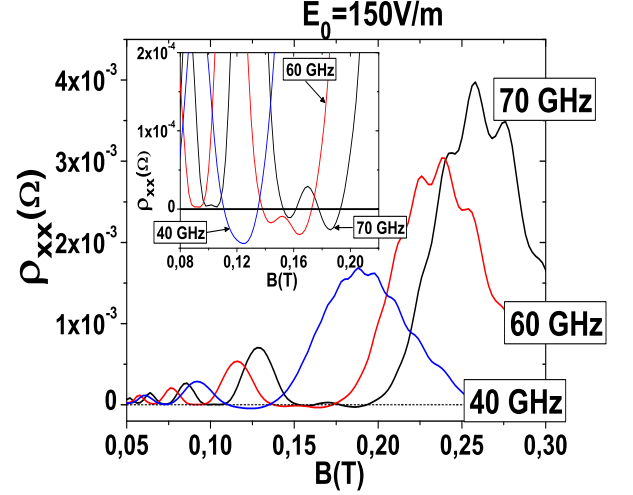


FIG. 3: Calculated magnetoresistivity ρ_{xx} as a function of B , for different frequencies at MW-intensity $E_0 = 150V/m$. In the inset we display a rising central peak in the middle of negative minimum that becomes positive as the MW-frequency is increased. Temperature: 500 mK.

at fixed MW-power. ANC is achieved for all the cases presented and the growth of the central peak as frequency is increased is clearly visible (see inset). The explanation is as follows. At constant E_0 , lower w corresponds to high values for the Bessel function arguments, i.e., J_0 's are decreasing and $J_{n \neq 0}$'s are increasing. In this regime, direct transitions (positive contributions) become less important than multi-photon, $J_n \rightarrow J_0$ transitions (negative contributions). The first ones are represented by the B_0 term in the scattering rate $W_{n,m}$ and σ_{xx} , and the second ones by B_1 and B_2 , (see Eqs. 2-5). Eventually the positive contributions are totally compensated by the negative ones and the central peak at minimum vanishes. As we increase the frequency, the reverse, occurs giving rise to a distinct positive peak in the middle of the negative minimum.

According to the model and calculated results presented above, high values for the ratio $\frac{E_0}{w}$ is a first and important condition to obtain photo-satellites and the consequent ANC. However this is not sufficient, and an additional condition has to be fulfilled concerning the external DC bias applied in the x direction, as we explain below.

In Fig. 4a we represent calculated ρ_{xx} versus B at fixed w and E_0 and at increasing external DC bias E_{DC} . We can observe at the two main minima how the ρ_{xx} negative values are shifted to positive as E_{DC} is raised. At the same time the central peak gets larger. The explanation can be seen from the schematic diagrams in Fig. 4b and 4c. In both cases we are in a regime where $\Delta X^{MW} < 0$. At lower bias (E_{DC1} , Fig 4.b), one-photon transitions giving negative current ($J_1 \rightarrow J_0$) dominate and, except

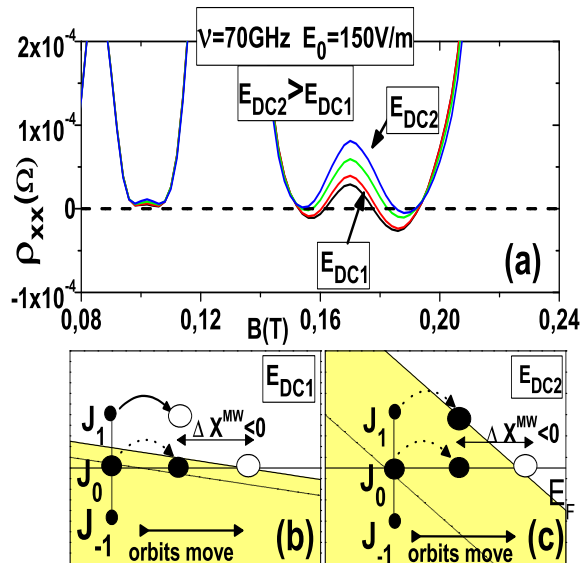


FIG. 4: (a) Calculated ρ_{xx} versus B at two minima for fixed MW-frequency and intensity and different external DC bias (E_{DC}). For increasing E_{DC} , ρ_{xx} minimum becomes positive. (b) Schematic diagrams explanatory for the lower bias case (E_{DC1}). In this situation the Fermi energy slope is smaller making the $J_1 \rightarrow J_0$ transitions predominant which provides negative contributions to the current. (c) Schematic diagram for higher bias (E_{DC2}). In this case the former $J_1 \rightarrow J_0$ negative contributions become positive because the final Landau state is now below the Fermi energy and therefore is not empty. As a result, most contributions are positive shifting the minimum of ρ_{xx} upwards and causing the central peak to increase. Temperature 500 mK.

in the central peak, they can compensate the positive direct ($J_0 \rightarrow J_0$) contributions. We observe that the final state for $J_1 \rightarrow J_0$ is well above the Fermi energy and the corresponding difference ($f_i - f_f$) > 0 , is important

making the negative contributions relevant. At higher bias E_{DC2} , we reach the situation depicted in Fig. 4c. The corresponding slope for the Fermi energy is larger than in the E_{DC1} case. Now the final state is below E_F , i.e., it is not empty making the corresponding difference ($f_i - f_f$) < 0 and the contribution to the current evolves from negative to positive. The final result is that the ρ_{xx} negative values get smaller for increasing E_{DC} becoming eventually zero or positive. Another important results is that the central ρ_{xx} peak becomes much larger which can be explained with similar arguments.

Therefore we can state that high values for $\frac{E_0}{w}$ and a regime of lower values for E_{DC} , constitute the two main conditions which have to be fulfilled in order to obtain ANC. Thus according to our theoretical model and taking into account of the experimental difficulties to measure negative resistance, we believe that by tuning the appropriate MW parameters and external DC bias, it would be possible to experimentally observe the evolution from ZRS to ANC.

In summary, we have presented here a theoretical model to explain the physics behind the existence of radiation-induced ANC in 2D electron systems. We are able to explain the transition from ZRS to ANC in terms of multi-photon assisted processes. It has also been shown how this transition can be tuned by the parameters of the microwave field. In addition, the external DC bias has been found to be of decisive importance in achieving ANC. We think that this work sheds some light on the controversy whether ANC actually occurs in these structures and which are the main parameters that govern the evolution from ZRS to ANC. The basic understanding of this process will be of importance to the future implementation of workable nanodevices.

We acknowledge Charles Creffield for the critical reading of the manuscript. This work was supported by the MCYT (Spain) grant MAT2002-02465, the ‘‘Ramon y Cajal’’ program (J.I.) and the EU Human Potential Programme HPRN-CT-2000-00144.

¹ F.Grossmann, T.Dittrich, P.Jung and P. Hanggi, Phys. Rev. Lett. **67**,516, (1991).
² R Lopez, R.Aguado, G.Platero and C.Tejedor, Phys. Rev. B, **64**,075319, (2001).
³ B.J. Keay et al., Phys. Rev. Lett. **75**,4098, (1995).
⁴ R.G. Mani, J.H. Smet, K. von Klitzing, V. Narayanamurti, W.B. Johnson, V. Umansky, Nature **420** 646 (2002).
⁵ M.A. Zudov, R.R. Du, N. Pfeiffer, K.W. West, Phys. Rev. Lett. **90** 046807 (2003).
⁶ R.G. Mani, V. Narayanamurti, K. von Klitzing, J.H. Smet, W.B. Johnson, V. Umansky, Phys. Rev. B **69** 161306(R) (2004).
⁷ R.G. Mani, Appl. Phys. Lett. **85**, 4962, (2004); R.G. Mani, Physica E, **22**, 1, (2004); R.G. Mani, Physica E, **25**, 189, (2004).

⁸ S.A. Studenikin, M. Potemski, A. Sachrajda, M. Hilke, L.N. Pfeiffer, K.W. West, Phys. Rev. B, **71**, 245313, (2005).; S.A. Studenikin, M. Potemski, P.T. Coleridge, A. Sachrajda, Z.R. Wasilewski, Solid State Comm **129**, 341 (2004).
⁹ C.L. Yang, M.A. Zudov, T.A. Knuttila, R.R. Du, L.N. Pfeiffer and K.W. West, Phys. Rev. Lett. **91**, 096803, (2003); M.A. Zudov, Phys. Rev. B, **69**, 041304, (2003).
¹⁰ R.R. Du, M.A. Zudov, C.L. Yang, L.N. Pfeiffer and K.W. West, Physica E, **22**, 7 (2004); R.R. Du, M.A. Zudov, C.L. Yang, Z.Q. Yuan, L.N. Pfeiffer and K.W. West, J. Mod. Phys. B, **18**, 3465, (2004).
¹¹ J.H.Smet, B. Gorshunov, C.Jiang, L.Pfeiffer, K.West, V. Umansky, M. Dressel, R. Dressel, R. Meisels, F.Kuchar, and K.von Klitzing, Phys. Rev. Lett. **95**, 116804 (2005).

- ¹² R.L. Willett, L.N. Pfeiffer and K.W. West, Phys. Rev. Lett. **93** 026804 (2004).
- ¹³ M.A. Zudov, R.R. Du, L.N. Pfeiffer and K.W. West, Phys. Rev. B, **73**, 041303 (2006).
- ¹⁴ A.C. Durst, S. Sachdev, N. Read, S.M. Girvin, Phys. Rev. Lett.**91** 086803 (2003)
- ¹⁵ C.Joas, J.Dietel and F. von Oppen, Phys. Rev. B **72**, 165323, (2005); J.Dietel, L.J. Glazman, F.W.J. Hekking and F. von Oppen Phys. Rev. B **71** 045329 (2005).
- ¹⁶ X.L. Lei, S.Y. Liu, Phys. Rev. Lett.**91**, 226805 (2003);
- ¹⁷ X.L. Lei, S.Y. Liu, Phys. Rev. B **72**, 075345 (2005);
- ¹⁸ V. Ryzhii and V. Vyurkov, Phys. Rev. B **68** 165406 (2003); V. Ryzhii, Phys. Rev. B **68** 193402 (2003); V.Ryzhii and R. Suris, J. Phys: Cond. Mat. **15**, 6855, (2003) ; Ryzhii et al, Sov. Phys. Semicond. **20**, 1299, (1986).
- ¹⁹ P.H. Rivera and P.A. Schulz, Phys. Rev. B **70** 075314 (2004)
- ²⁰ Junren Shi and X.C. Xie, Phys. Rev. Lett. **91**, 086801 (2003).
- ²¹ Kang-Hun Ahn, J. Korean Phys. Soc., **47** (4), 666-672, (2005).
- ²² A.V. Andreev, I.L. Aleiner and A.J. Millis, Phys. Rev. Lett. **91**, 056803 (2003)
- ²³ J. Iñarrea and G. Platero, Phys. Rev. Lett. **94** 016806, (2005)
- ²⁴ T-K Ng and Lixin Dai, Phys. Rev. B, **72**, 235333 (2005).
- ²⁵ J. Iñarrea and G. Platero, Phys. Rev. B **72** 193414 (2005)
- ²⁶ J.Iñarrea, G. Platero and C. Tejedor, Phys Rev. B. **50** 4581, (1994).
- ²⁷ J.Iñarrea and G. Platero Phys Rev. B. **51** 5244, (1995).
- ²⁸ E.H. Kerner, Can. J. Phys. **36**, (3) 371-377 (1958) .
- ²⁹ K. Park, Phys. Rev. B **69** 201301(R) (2004).
- ³⁰ B.K. Ridley. Quantum Processes in Semiconductors, 4th ed. Oxford University Press, (1993).